Catalysis Communications 11 (2010) 408–413

Contents lists available at ScienceDirect

Catalysis Communications

journal homepage: www.elsevier.com/locate/catcom

Optimization of manganese content by high-throughput experimentation of $Pt/WO_x–ZrO_2–Mn$ catalysts

M.L. Hernandez-Pichardo [a], J.A. Montoya de la Fuente [b,*], P. del Angel [b], A. Vargas [b], I. Hernández [c], M. González-Brambila [c]

[a] Instituto Politécnico Nacional, ESIQIE, Laboratorio de Catálisis y Materiales, Av. IPN S/N Zacatenco, 07738 México, Mexico
[b] Instituto Mexicano del Petróleo, DIyP, Eje Central Lázaro Cárdenas Norte 152, 07730 México D.F., México
[c] Universidad Autónoma Metropolitana, División de CBI, Av. San Pablo 180 Col. Reynosa, 02200 México D.F., México

ARTICLE INFO

Article history:
Received 27 August 2009
Received in revised form 6 November 2009
Accepted 11 November 2009
Available online 16 November 2009

Keywords:
Tungstated zirconia
Manganese
n-Hexane hydroisomerization
High-throughput experimentation

ABSTRACT

A library of $Pt/WO_x–ZrO_2–Mn$ catalysts was developed in order to optimize the manganese content in this catalytic system for the isomerization of *n*-hexane. The catalysts were synthesized, characterized and screened using high-throughput experimentation (HTE) techniques. The catalysts were prepared by surfactant-assisted coprecipitation whereas the characterization was done by X-ray diffraction (XRD), Raman and UV–vis spectroscopy. For this second screening, several catalysts with different manganese contents were prepared; it was found that the incorporation of Mn modifies the anchorage of tungsten on the zirconia surface, thus improving its catalytic properties, in terms of the *n*-hexane conversion and selectivity, depending on the catalyst composition. These results suggest that this methodology allows the optimization of manganese and tungsten contents on these solid catalysts.

1. Introduction

Solid acids, such as sulfated zirconia (SZ) and tungstated zirconia (WZ) catalysts have been thoroughly studied as an environmentally friendly alternative for the current isomerization processes. The catalytic properties of these solids can be improved by the addition of some promoters such as Fe, Mn, and/or Cr [1,2], Al [3,4], or Ce [5]. Particularly, in the case of tungstated zirconia, several authors have studied the effect of doping these catalysts trying some others metals like Ga or Al [6–8], and have pointed out the importance of adding promoters to this system in order to improve the catalytic performance of these materials. However, it was found that although Fe and Mn promote sulfated zirconia for *n*-alkenes isomerization, they do not promote tungstated zirconia due to the formation of Mn or Fe tungstates that hinders the promoter effect of these components [9].

In the case of sulfated zirconia, the promoting effect of Mn, Fe and others ions has been attributed to many factors. Some of these factors include the stabilization of carbenium ion and alkene intermediates on the surface, the increase in the dehydrogenation ability, the improvement of the dispersion of the active species on the surface or the preferential incorporation of some cations into the zirconia lattice [10]. It has also been suggested that the promoting effect of these metals is a combination of several factors, including decoration of platinum with oxides, favoring the migration of the activated species, modifying the reducibility of the tungsten phase [8], increasing the stability of the tetragonal zirconia or modifying the domain size of the WO_x species on the surface [11]. The promoting effect of Al or Ga for instance, was also suggested to be a combination of several factors, such as the stability of the tetragonal zirconia structure, the modification of the crystallite size of WO_3 on the surface of WZ or the improvement of the redox properties of W^{6+} [6].

Despite of all the efforts focused to the understanding of the promoter role, there is still some controversy about the catalytic effect of these metals. Particularly for Fe and Mn, some research about the individual role of these promoters is necessary. In this work, the influence of the manganese content on the nanostructure and reactivity of $WO_x–ZrO_2$ materials was studied. This study is a continuation of previous works on $Pt/WO_x–ZrO_2–Mn$ catalysts [11,12] where we developed a primary study for the leads discovery in tungsten composition, pre-treatments and precursors. We reported that the catalytic properties depend on the dispersion of the tungstated phase and those results suggested that the incorporation of Mn modifies the properties of the surface WO_x species. However, the specific effect of the Mn addition was not very clear. We therefore prepared a new series of $Pt/WO_x–ZrO_2–Mn$ materials with different manganese contents in order to evaluate the effects of Mn over the catalytic performance, and to optimize the content of this ion by using HTE techniques, since these approaches allow the comparison of the catalytic behavior under identical conditions.

* Corresponding author. Tel.: +52 55 91758375.
E-mail address: amontoya@imp.mx (J.A. Montoya de la Fuente).

1566-7367/$ - see front matter © 2009 Elsevier B.V. All rights reserved.
doi:10.1016/j.catcom.2009.11.010

2. Experimental

2.1. Catalysts preparation

High-throughput experimentation techniques were applied to the synthesis of a library of 24 Pt/WO_x–ZrO_2–Mn catalysts, with different manganese (0, 0.5, 1 and 2 wt.%), tungsten (10, 15 and 20 wt.%) and surfactant contents. Catalysts were prepared by surfactant-assisted coprecipitation method, as it was previously reported [11]. Briefly, the Multicomponent Pt/WO_x–ZrO_2–Mn catalyst library has been synthesized using Cavro robots (model MSP 9500 by Symyx) in an automated parallel synthesis. Hydrous zirconia was coprecipitated with tungsten, Mn and surfactant solutions that were prepared from zirconyl chloride, ammonium metatungstate, manganese nitrate, and cetyl-trimethylammonium bromide (CTAB), respectively, all from Aldrich. The precipitates were washed several times with deionized water, and the resulting paste was dried at 110 °C overnight, and then calcined at 800 °C for 4 h.

These samples were labeled as Mn(x)W(y)Z–S, where x and y are the Mn and W concentrations in wt.% respectively, and S = Surfactant/ZrO_2 molar ratio employed (0 or 2). For platinum impregnation (0.3 wt.%), the vials of the library plate were filled with the WO_x–ZrO_2–Mn powders, and a $H_2PtCl_6{\cdot}6H_2O$ (Aldrich) aqueous solution was dispensed onto the samples by the pipetting robot system. Then the solvent was evaporated and the remaining coating on the samples was dried at 110 °C overnight and finally calcined at 400 °C for 3 h. In analogy with previous nomenclature, the resulting materials were denoted as Pt/Mn(x)W(y)Z–S, indicating that the materials were impregnated with platinum.

2.2. Catalytic testing

Catalytic activity was measured in the n-hexane hydroisomerization reaction over the Pt/WO_x–ZrO_2–Mn catalysts. The evaluation was carried out in a Combinatorial Multi Channel Fixed Bed Reactor (MCFBR) (Symyx, Tech) fully automated, evaluating 48 samples in parallel. A catalyst sample of 100 mg diluted with 200 mg of inert silicon carbide was loaded in each well and fixed into the reactor heads, containing a set of eight micro-reactors of approximately 4 mm of inner diameter and 47 mm in length. The six reactor heads are connected independently to six chromatographs (Agilent, 6850 Series) each one equipped with a SPB-1 capillary column (Supelco) with a length of 100 m, and a flame ionization detector (FID) for the analysis of products. The injection of the reactant and products to the GCs was carried out at the reaction pressure. The reliability of the quantitative method was evaluated with an uncertainty of the conversion ±2% measurable through the 48 wells. The pretreatment of the catalysts was carried out in situ prior to the activity test. It comprised a drying-reduction program, drying the samples at 260 °C for 2 h in helium (200 cm^3 min^{-1}) followed by reduction in a hydrogen flow (200 cm^3 min^{-1}) at 450 °C for 3 h. Hydrogen and n-hexane flows were adjusted to give a $H_2/n\text{-}C_6$ = 1.47 M ratio. The reaction was conducted at 260 °C, 0.689 MPa, 3.7 h^{-1} WHSV using a mixture of 100 cm^3 min^{-1} H_2 and 0.4 cm^3 min^{-1} of n-hexane fed with an HPLC pump.

2.3. Catalyst characterization

WO_x–ZrO_2–Mn nanostructured mixed oxides were characterized by X-ray powder diffraction (XRD), UV–vis, and Raman spectroscopy. The WO_x–ZrO_2–Mn materials were characterized without Pt since in this study only the quantity of sample needed for the catalytic evaluation (100 mg) was impregnated with Pt with the aim of not wasting this expensive metal. X-ray diffraction patterns were obtained in a Bruker-Axs D8 Discover with GADDS (General Area Detector Diffraction Systems, two-dimensional detector) diffractometer fitted with a Cu tube (40 kV, 40 mA) using HTE approaches for both, measurements and patterns evaluation. Ultraviolet–visible (UV–vis) spectra were obtained using a Varian (Cary 1G) spectrophotometer for the data handling with an integration sphere accessory. Finally, Raman spectra were recorded in the 100–1200 cm^{-1} wave number range using a ThermoNicolet Raman apparatus (Almega model) equipped with a Nd:YVO4DPSS laser source. The excitation line of the laser was 532 nm and the laser power was of 25 mW.

3. Results and discussion

In previous works dealing with the improvement of catalytic performance of Pt supported on tungstated zirconia materials dopped with manganese [11,12], we have studied the effects of the main variables that affect the catalytic activity of these materials on isomerization processes. We found the method, composition, precursor and pre-treatments that lead to a higher catalytic performance. However, as far as the manganese doping is concerned, we found that the incorporation of 1% of Mn yields different behaviors, depending on the tungsten dispersion on the zirconia surface [11]. Thus, in this secondary screening we have focused our study on the optimization of the manganese content by allowing parallel testing to obtain high conversions and selectivity towards the bi-ramified isomers.

3.1. Catalytic activity

The catalytic activity of these materials was evaluated in the n-hexane hydroisomerization reaction at 260 °C; the general results are shown in Fig. 1. These results show the influence of the Mn content on the n-hexane conversion of Pt/WO_x–ZrO_2–Mn catalysts as a function of tungsten loadings and surfactant content. It is observed that the catalytic activity of samples without Mn increases according with the increment of tungsten content from 10% to 20% in both cases: without surfactant (S = 0) and with surfactant (S = 2). In general, it is observed that the surfactant improves the catalytic activity of these materials. On the other hand, when Mn is incorporated into the catalytic system it is observed as general tendency that as the tungsten concentration increases the catalytic activity decreases for every individual concentration of Mn, being the highest conversions at low Mn concentrations. One possible explanation is that at low Mn concentrations (0.5% Mn) this ion acts as a dopant and it is highly dispersed, thus it can be located on the support but also on the WO_x clusters modifying the WO_x anchorage and therefore the catalytic activity. As the Mn concentration increases, it begins to form MnO_x nanocrystals that go preferentially to the zirconia support and the effect over the WO_x active sites is less intense. From these results, it is clear that the behavior of catalysts doped with Mn is very different from those catalysts without Mn, since in the last ones the catalytic activity increases with the W content, whereas the doped catalysts show an inverse behavior. It is also possible that the small differences between real and nominal compositions, as well as differences in surface area are changing the catalytic results; however, the tendencies indicate that the variations are similar for all the catalysts. It is also observed that the addition of this cation promotes mainly the activity of samples with low tungsten content (10% W). In the case of samples without surfactant (S = 0), the manganese presents a promoter effect only in samples with low tungsten content (10–15% W). This result suggests that the incorporation of manganese to this catalytic system allows the optimization of the tungsten content, since the addition of only 0.5% Mn increases the conversion catalyst with low tungsten content by 50% mol. It is important to mention that in this

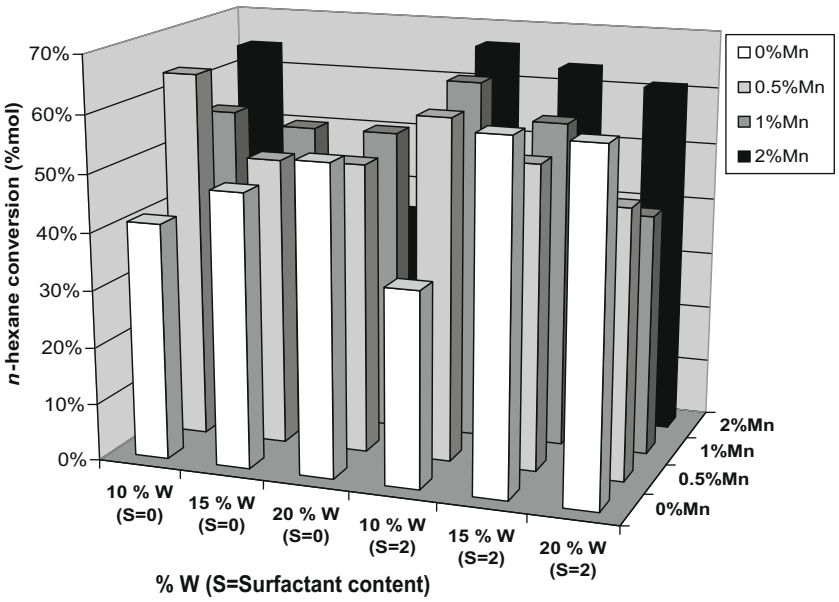

Fig. 1. Secondary screening for the catalytic performance in the *n*-hexane isomerization reaction at 260 °C of Pt/WO_x–ZrO_2–Mn catalysts at different manganese and tungsten loadings.

work, the Pt content was maintained constant (0.3 wt.%) keeping the amount of Pt used industrially since the most important role of platinum is to stabilize the catalytic activity [13].

Moreover, as we expected, the preparation of the catalysts using surfactant produces an increase in the catalytic activity of these materials. As we have previously reported [14], the rise on the surfactant content on this type of samples generates modifications in the mesoporosity, as well as an increase in its specific area, which produces modifications on the WO_x dispersion and thus on the catalytic performance of these materials. Some N_2 physisorption analysis were performed on the Mn(1)W(15)Z-0 and Mn(1)W(15)Z-1 catalysts, in order to confirm these trends. From these analysis, isotherms type IV (not showed) with the hysteresis loop characteristic of mesoporous materials with open pores systems were obtained for both catalysts, but the surface area for the catalysts prepared with surfactant (Sg = 90.3 m^2/g) was higher than the catalysts without surfactant (Sg = 70.6 m^2/g).

In addition, Table 1 shows the conversion and selectivity obtained in the *n*-hexane isomerization reaction for blank catalysts (manganese and surfactant free) as well as the lead catalysts. Comparison of the conversions and selectivity of the lead samples shows that the most active catalysts were materials prepared with manganese and low contents of tungsten, or with 20% W prepared with surfactant. It is also possible to observe that all the catalysts presented the formation of the four isomers: 2-methyl-pentane (2 MP), 3-methyl-pentane (3 MP), 2,2-dimethyl butane (2,2 DMB) and 2,3-dimethyl butane (2,3 DMB). It was found that the addition of Mn improves the selectivity to the secondary bi-ramified isomers, of higher octane number, in catalysts with low tungsten content (10% W). Particularly, the increase in the 2,2-dimethyl butane product which is a secondary product indicates an increase in the activity of the Mn-containing catalysts. The explanation of this behavior is the reaction mechanism; according to most accepted mechanism (Scheme 1) both methylpentanes (2 MP and 3 MP) are primary products, while 2,2 DMB and 2,3 DMB are secondary products, but 2,3 DMB approaches rapidly to equilibrium.

Some authors have suggested that the role of manganese as dopant in Fe and Mn sulfated zirconia catalysts (FMSZ) might be to raise or stabilize the dispersion of the Fe [10,15]. According to the results obtained in this work, we suggest that the promoter effect of manganese is generated when the Mn is incorporated into the zirconia and modifies the interactions between the polytungstate species and the zirconia. It allows the formation of well-dispersed WO_x species on suitable sizes to form the active sites for the isomerization of the alkane. However, when the tungsten content is higher, the addition of a higher content of Mn (2% for instance)

Table 1
Conversions and products distribution for blank and lead catalysts in the *n*-hexane isomerization reaction at 260 °C.

Catalyst	X_A (% mol)	2,2 DMB	2,3 DMB	2 MP	3 MP	Cracking
Pt/W(10)Z	41.4	3.2	12.1	49.7	32.9	1.3
Pt/W(15)Z	47.9	3.6	12.8	48.9	32.0	2.0
Pt/W(20)Z	54.0	4.3	12.0	49.6	32.9	0.7
Pt/Mn(0.5)W(10)Z-0	64.2	5.1	12.2	49.1	32.4	0.7
Pt/Mn(1)W(10)Z-0	55.0	4.3	12.05	49.7	33.5	0.5
Pt/Mn(2)W(10)Z-0	64.4	5.2	12.9	48.8	31.6	1.5
Pt/Mn(0)W(15)Z-2	60.6	4.9	12.5	48.4	31.3	2.4
Pt/Mn(0)W(20)Z-2	60.3	4.5	12.1	49.1	32.7	1.1
Pt/Mn(0.5)W(10)Z-2	59.7	4.5	12.4	48.8	32.2	2.1
Pt/Mn(1)W(10)Z-2	63.0	5.0	11.8	49.5	32.7	1.0
Pt/Mn(2)W(10)Z-2	66.7	6.4	11.6	48.7	31.9	1.0
Pt/Mn(1)W(15)Z-2	56.9	4.7	12.4	48.9	32.1	1.9
Pt/Mn(2)W(15)Z-2	63.6	5.2	11.7	49.3	32.5	0.8
Pt/Mn(2)W(20)Z-2	61.2	4.5	12.9	47.7	31.0	3.7

$$n-C_6 \Leftrightarrow \begin{matrix} 2-MP \\ \Updownarrow \\ 3-MP \end{matrix} \Leftrightarrow 2,3DMB \Leftrightarrow 2,2DMB$$

Scheme 1. *n*-Hexane isomerization mechanism.

is necessary. In this regard, Iglesia and his group [16] have suggested that the activity of WO_x–ZrO_2 catalysts depends on the size of the WO_x species developed on the zirconia surface. If the tungsten surface density is lower than 4 W nm^{-2}, they will generate a strong interaction with the support, while in larger crystals most of the active sites are founded in the bulk of the cluster. This could also explain the difference between the catalytic activity of materials with different compositions, since, if there is an excess or a deficiency of manganese, depending on the tungsten content, the promoting effect of this cation is not generated. This effect is clear on catalysts with 10% of W, since the activity of these samples was promoted by the addition of manganese, even with low manganese content.

3.2. Catalysts characterization

In regards to the characterization of the WO_x–ZrO_2–Mn samples by XRD (Fig. 2), we found that these samples are formed mainly by the tetragonal zirconia phase and monoclinic tungsten oxide (WO_3). These diffraction patterns were measured simultaneously under the same conditions using a HTE approach; therefore, the patterns can be directly compared, as well as the reflection positions and intensity. The diffraction patterns for samples prepared without surfactant ($S = 0$) are shown in Fig. 2a. These patterns indicate that the tungsten oxide is well dispersed, since the WO_3 crystalline phase ($2\theta = 23.3$–24.4) is only observed in samples with high tungsten content and low manganese content. The overall analysis of these patterns indicates that the increase in the manganese content improves the dispersion of the WO_x phase, since at higher Mn contents the diffractions corresponding to the WO_3 diminishes or they are not detected. This result reveals that the polytungstate species developed on the surface are smaller than WO_3 crystals and the fact that they are not observed by XRD indicates that these nanostructures have a domain size smaller than 3 nm with a tungsten surface density lower than 10 W nm^{-2}. It also suggests that the inclusion of Mn to the tungstated zirconia modifies the anchorage of the tungstated species and the mechanism by which these structures are developed on the zirconia surface.

On the other hand, in samples prepared with surfactant (Fig. 2b) most of the samples with 15% and 20% of tungsten, show diffraction peaks corresponding to the formation of the crystalline monoclinic WO_3 phase, with low intensity due to the higher dispersion produced by the effect of surfactant, which generates an increase in the surface area. The effect of the incorporation of Mn on the dispersion of the WO_x clusters is less evident due to the addition of surfactant; however, from the diffractograms of Fig. 2b is also possible to observe a slower growth of these species to the formation of the crystalline phase of WO_3 with the increase in the Mn concentration. These results along with the catalytic activity suggest that a high activity requires the formation of well-dispersed WO_x species.

However, the activity of these catalysts cannot be explained considering only the stabilization of the different phases observed by XRD, therefore, spectroscopic techniques were used to identify not segregated tungsten species on the zirconia surface. The effect of the addition of manganese to these catalysts is shown in Fig. 3.

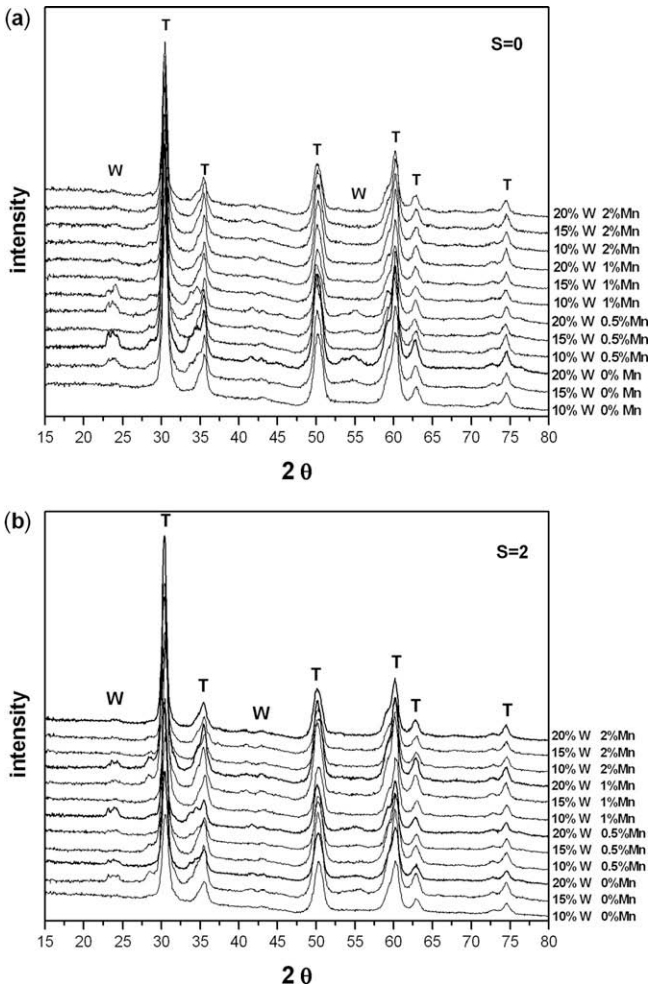

Fig. 2. XRD spectra for WO_x–ZrO_2–Mn samples: T = tetragonal zirconia, W = WO_3. (a) Effect of the Mn incorporation, and (b) effect of the surfactant and manganese.

This figure shows as an example, the Raman spectra of samples with 15% W at different manganese contents, prepared without surfactant. These spectra present the characteristics bands of crystalline WO_3 with low intensity and a slight shift to lower frequencies at 260 and 312 cm^{-1}, that correspond to W–O–W deformation modes, and 706 and 798 cm^{-1} corresponding to W–O bending and stretching modes, respectively [16]. The spectra also show the presence of a band at about 970 cm^{-1} that is characteristic of the octahedrally coordinated polytungstate species with terminal W=O bonds [17]. The presence of these bands indicates that different tungstated species are formed in the zirconia surface, from small oligomeric WO_x clusters to the formation of WO_3 crystallites. Moreover, it is observed that at the manganese content increases, the bands become less intense, with the same tungsten content, suggesting that the surface WO_x density decreases in agreement with the XRD results. It is important to mention that these spectra correspond to samples prepared without surfactant, so that the effect shown is attributed only to the manganese incorporation. As it has been previously reported [18], Raman scattering cross sections for crystalline WO_3 are much greater than for surface polytungstate species; thus, the bands corresponding to WO_3 dominate the spectra, even when the polytungstate clusters are the most abundant surface structures.

Finally, the UV–vis spectra recorded in air also suggest that manganese produces a modification on the surface WO_x nanostructure. Fig. 4 compares the UV–vis spectra for samples with 10% of

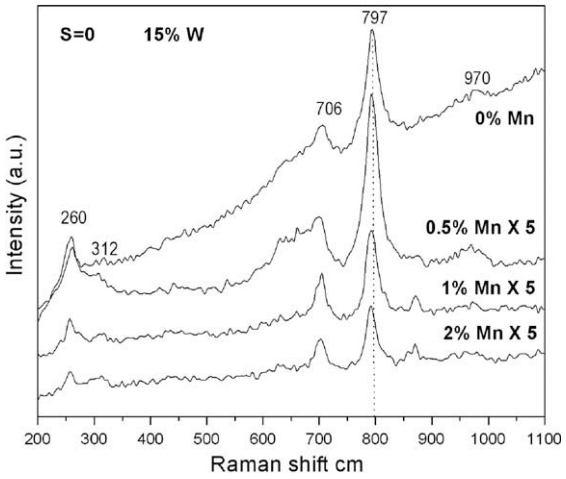

Fig. 3. Raman spectra of some WO_x–ZrO_2–Mn samples with 15% W and different manganese contents.

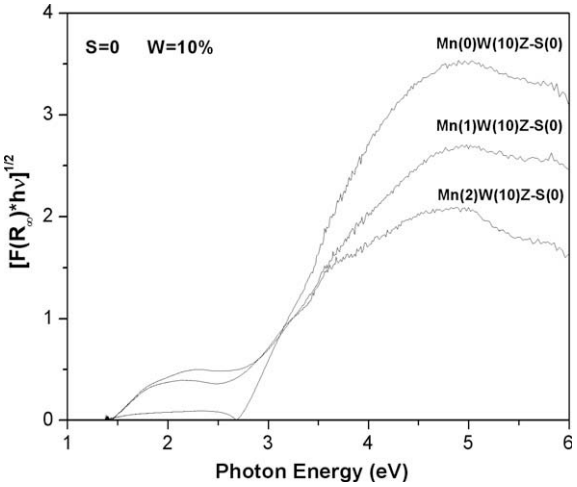

Fig. 4. Diffuse reflectance UV–vis absorption spectra of WO_x–ZrO_2–Mn samples with 10% W and different manganese contents.

tungsten loading and different manganese contents. These spectra present a broad absorption band between 3 to 5 eV, corresponding to different $O^{2-} \rightarrow W^{6+}$ electronic transitions, according to literature [19], overlapped with the absorption corresponding to the ZrO_2 at about 4–5 eV with almost the same intensity. It is observed that as the manganese content increases, the intensity of the absorption band decreases, which suggests a slight reduction of the tungsten surface density in catalysts with the same tungsten concentration. This decrease in the absorption band intensity is similar to that produced for the decrease of the tungsten loading in tungstated zirconia catalysts [16], with a slight reduction of the edge energy (E_0) towards lower energy values, from 2.7 to 2.4 eV. Therefore, this behavior in catalysts with the same tungsten content could indicate that the Mn incorporation facilitates the ligand-to-metal charge transfers of tungsten species. This could explain the improved performance in catalysts prepared with Mn in samples with low tungsten content, since in these samples the tungsten surface density is low (according to XRD results). These isolated WO_x species present a strong interaction with the zirconia, and they are difficult to be reduced. Further, the addition of Mn makes weaker this interaction facilitating the reduction of the clusters and the formation of the Brönsted acid sites according to the mechanism proposed by Barton et al. [16] for the formation of these sites on ZW catalysts.

In summary, we observed in this work that the use of Mn as promoter modifies the nanostructure and WO_x–ZrO_2 interactions of tungstated zirconia catalysts. These nanocrystalline structures exhibit properties different from those observed in microcrystalline structures, facilitating the reduction of the WO_x clusters and the formation of the acid sites mainly in catalysts with low tungsten content. This result indicates that by means of the incorporation of a low quantity of Mn, it is possible to optimize the tungsten loading on Pt/WO_x–ZrO_2 catalysts. On the other hand, the reactivity depends not only on the reducibility but also on the accessibility of the WO_x species on the zirconia surface, because the tungsten species must be first expelled from the bulk before they form the active WO_x sites, being the main effect of the surfactant on the high performance of these catalysts.

These results show the importance of the high-throughput experimentation because the catalytic activity is not a linear function of the tungsten content against the Mn concentration, and only using HTE is possible to measure many different concentrations, which would be very difficult to do by traditional experimentation.

4. Conclusions

A secondary screening for the study of Pt/WO_x–ZrO_2–Mn catalysts was performed in order to optimize the manganese and tungsten contents in this catalytic system. It was found that the incorporation of Mn to tungstated zirconia catalysts modifies the anchorage of the tungstated species on the zirconia surface. The promoting effect of manganese on this system is generated when this cation is incorporated into the zirconia lattice and modifies the interaction between tungsten and zirconia, thus forming WO_x clusters of suitable domain size to be easily reduced to form active sites. In addition, the use of a surfactant produces a higher expel of the WO_x species from the bulk to generate more active sites, as well as an increase in the surface area that modify the tungsten surface density and the interaction with the zirconia surface developing an acid character. These results show the importance of the high-throughput experimentation because in some catalytic systems the catalytic behavior is not a linear function of the compositions, and only using HTE is possible to measure many different concentrations, which would be very difficult to do by traditional experimentation.

Acknowledgements

M.L.H.P. would like to acknowledge to the Instituto Politécnico Nacional (IPN) for the financial support received. We thank the facilities of the Combinatorial Catalysis and Electron Microscopy Laboratories of the Instituto Mexicano del Petroleo. The authors also thank Prof. Ricardo Macias Salinas for the revision of the Manuscript.

References

[1] J.E. Tábora, R.J. Davis, J. Catal. 162 (1996) 125–133.
[2] J.A. Moreno, G. Poncelet, Appl. Catal. A 210 (2001) 151–164.
[3] A. Barrera, J.A. Montoya, M. Viniegra, J. Navarrete, G. Espinosa, A. Vargas, P. del Angel, G. Pérez, Appl. Catal. A 290 (2005) 97–109.
[4] Ch. Hwang, X. Chen, S. Wong, Ch. Chen, Ch. Mou, Appl. Catal. A 323 (2007) 9–17.
[5] A. Corma, J.M. Serra, A. Chica, Catal. Today 81 (2003) 495–506.
[6] X.R. Chen, Ch.L. Chen, N.P. Xu, Ch.Y. Mou, Catal. Today 93 (2004) 129–134.
[7] J.G. Santiesteban, D.C. Calabro, C.D. Chang, J.C. Vartuli, T.J. Fiebig, R.D. Bastian, J. Catal. 202 (2001) 25–33.
[8] P. Lukinskas, S. Kuba, B. Spliethoff, R.K. Grasselli, B. Tesche, H. Knözinger, Top. Catal. 23 (2003) 163–173.

[9] M. Scheithauer, R.E. Jentoft, B.C. Gates, H. Knözinger, J. Catal. 191 (2000) 271–274.
[10] F.C. Jentoft, A. Hahn, J. Kröhnert, G. Lorenz, R.E. Jentoft, T. Ressler, U. Wild, R. Schlögl, C. Häßner, K. Köhler, J. Catal. 224 (2004) 124–137.
[11] M.L. Hernandez-Pichardo, J.A. Montoya, P. del Angel, A. Vargas, J. Navarrete, Appl. Catal. A 345 (2008) 233–240.
[12] M.L. Hernandez-Pichardo, J.A. Montoya de la Fuente, P. Del Angel, A. Vargas, C. Reza, Cat. Comm. 10 (2009) 1828–1834.
[13] Y. Ono, Catal. Today 81 (2003) 3–16.
[14] M.L. Hernández, J.A. Montoya, I. Hernández, M. Viniegra, M.E. Llanos, V. Garibay, P. Del Angel, Micropor. Mesopor. Mater. 89 (2006) 186–195.
[15] E.A. García, E.H. Rueda, A.J. Rouco, Appl. Catal. A 210 (2001) 363–370.
[16] D.G. Barton, M. Shtein, R.D. Wilson, S.L. Soled, E. Iglesia, J. Phys. Chem. B 103 (1999) 630–640.
[17] J.R. Sohn, M.Y. Park, Langmuir 14 (1998) 6140–6145.
[18] S.S. Chan, I.E. Wachs, L.L. Murrell, J. Catal. 90 (1984) 150–155.
[19] A. Gutiérrez-Alejandre, J. Ramírez, G. Busca, Langmuir 14 (1998) 630–639.